

New Calculation of Charge Generation Efficiency and Photocurrent in Organic Photoconducting Device

Choongkeun Lee, Jin-Woo Oh, Chil-Sung Choi, Nam-Soo Lee,^{†,*} and Nakjoong Kim*

Department of Chemistry, Hanyang University, Seoul 133-791, Korea

[†]Department of Chemistry, Chungbuk National University, Cheongju 361-763, Korea. *E-mail: nslee@chungbuk.ac.kr

Received July 25, 2008, Accepted November 11, 2008

A new approach was applied to examine the charge generation and transport in organic photoconductive devices by Monte-Carlo simulation utilizing multiple site interactions of carriers with all other charges within Coulomb radius. Stepwise generation frame was considered first by a charge separation process that was counted in two separate transactions, i.e., hopping against physical decay and dissociation against recombination. Thereafter, diffusion/drift process of free carriers was counted to follow. This method enables to examine readily the photocurrent generated alongside the charge generation efficiency. The field and temperature dependences of the efficiency and photocurrent were obtained comparable to Onsager's and experimental data.

Key Words: Monte Carlo simulation, Photo charge generation, Photocurrent, Multiple site interaction

Introduction

The photoconductivity phenomena have been investigated through the photo charge generation by illumination of the light.¹⁻⁹ The mechanism of free charge generation was explored theoretically by Onsager with his geminate recombination theory.⁹ In his model, a free charge is generated when the separation distance of the geminate pair created in the initial separation process becomes infinity. When the distance of two opposite charges initially separated is zero, the charges are diminished by geminate recombination. These competitive processes are represented by relative Brownian motions.^{1,2,6,9,10,11}

In Onsager's model, the electron-hole pair recombination was sometimes inappropriate for experimental data because the lifetime of the metastable state of a charge transfer (CT) complex is typically 10^{-8} s.³ Braun suggested, instead, a kinetic model in which the free charge generation probability was determined by the product of dissociation rate constant and the lifetime of the metastable state of a CT complex.³ In his model, the dissociation rate constant effectively depended on the applied field. The prediction curves for the field dependence of free charge generation for CT radii of 5 Å to 10 Å were generally in agreement with experimental results.

Melz investigated the application of Onsager's theoretical prediction to the electric field dependence under a two-step generation framework.¹ He reported that the initial separation process depended on the sample compositions. Borgenger and his group showed the thermalization distance, i.e., the initial separation distance, was independent of temperature and determined by the excitation wavelength through the comparison of the photo charge generation of poly(*N*-vinylcarbazole) with Onsager's theory.² To obtain the best fit for experimental data of the photo charge generation for poly(*N*-vinylcarbazole), the assumption of the Gaussian distribution for initial separations of excited elec-

tron-hole pairs turned out to be effective.^{4,5} Theoretical approaches based on Onsager's model have advantages in dissociation of geminate pairs, but have limitations in explaining the chemical effects in terms of molecular properties of materials in photorefractive films. Another theoretical approach utilizes the Monte-Carlo (MC) simulation.¹²⁻¹⁸ Bäessler and his group had studied the yield of geminate pair dissociation using the MC method. They reported that the disorder in energy helped the dissociation process and gave rise to a sub-Arrhenius-type temperature dependence for the yield.^{12,13} The photo charge generation process was usually explained by a two-step process. In the first step, the absorbed photons excite electrons in the CT complex from its ground state to an excited state. In the second step, the empty hole at the ground state is filled by radiative and/or non-radiative decay processes or by an electron hopping process from a neighboring charge transfer site to generate a geminate electron-hole pair.^{1,3,4,7}

In this paper, we tried a new approach to examine the photo charge generation and photocurrent at the same time using the MC method employing the multiple site generation, and counting the multiple site interaction. Carriers generated at homogeneously dispersed sensitizer sites can perform attractive or repulsive interactions between the mobile hole and neighboring charges during drifting through the matrix. The schematic of multiple site interaction is described in Fig. 1. A hole dissociates from a geminate pair, and moves toward a cathode driven by an applied field resulting in drifting, or recombines with an electron through geminate or distant-pair(non-geminate) recombination processes. The recombination immediately extinguishes an electron-hole pair. The field and temperature dependences of the photo charge generation efficiency and the photocurrent were examined by this method and compared to experimental data and previous theoretical studies of Onsager's. The sensitizer concentration dependence of the photocurrent was also acquired from calculations.

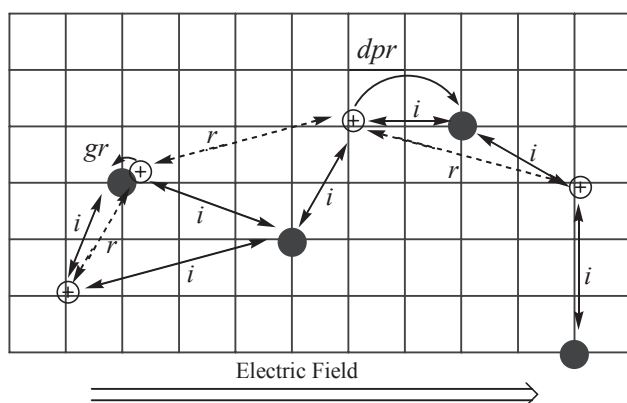


Figure 1. Scheme of multiple site generation and interaction, where $\bullet\oplus$; geminate electron hole pair, \bullet ; electrons, \oplus ; free holes, gr ; geminate recombination process, dpr ; distant-pair(non-geminate) recombination process, i ; inductive effect, and r ; repulsive effect.

Simulation and Experimental Details

The MC simulations were performed on a cubic lattice of $70 \times 50 \times 50$ sites ($x \times y \times z$). The periodic boundary condition was introduced along the x , y and z axes. The lattice sites were assigned randomly and homogeneously as either a sensitizer (generation) site of 1% or a hole conducting site of 99%. Randomly oriented and uncorrelated dipole moments \vec{p} are assumed to be placed at each lattice site. The dipole moment of molecules adapted in the simulations was calculated at B3LYP levels of theory using 6-311G** basis set with the Gaussian program package (Gaussian, Inc.). Calculated dipole moments of 2,4,7-trinitro-9-fluorenone (TNF) and monomer of poly[methyl-3-(9-carbazolyl)-propylsiloxane] (PSX-Cz) were 1.25 D and 2.44 D, respectively.

The energy of a hopping site was assumed to be the Ewald sum of its interactions with dipoles at all neighboring sites except its own.^{19,22,23} A hundred configurations of the site energies were sampled to obtain meaningful statistics. The hopping rate v_{ij} , from site i to j was adapted from the Miller-Abrahams theory,^{12,14-17,24,25}

$$v_{ij} = v_0 \exp(-\gamma|r|) \begin{cases} \exp[-\Delta\varepsilon/kT]; & \Delta\varepsilon > 0 \\ 1 & ; \Delta\varepsilon < 0 \end{cases}$$

where r denotes the distance between site i and j , and γ the wavefunction overlap parameter. The distance r was adjusted by a lattice constant, $r = r_{ij}(a_i + a_j)/2$, where r_{ij} denotes the distance between site i and j when the lattice constant was 1.0. The lattice constant was 1.0 for the transport site and 2.0 for the generation site. The wavefunction overlap parameter γ was expressed by $\gamma = (\gamma_i + \gamma_j)/2$, where $\gamma_i = 10a_i$. The intrinsic rate parameter was set to $v_0 = 1 \times 10^{13}$ /s. The energy difference under generated SCF was defined as $\Delta\varepsilon \equiv \varepsilon_j - \varepsilon_i - e \int_{x_i}^{x_j} \vec{E}(x) dx$ where ε_i and ε_j are the site energies, \vec{E} the modulated electric field, and e the elementary charge. To perform multiple site interactions, the energy gap between site i and j was adjusted by Coulomb interactions with charges occupied in the Coulomb radius. Throughout the simulation, the field was recalculated by Poisson's equation. Other conditions may be

referred to in our previous studies.¹⁹⁻²¹

The irradiation of 700 nm photons at 0.1 w/cm^2 was used in this simulation. The illuminated photons were absorbed by the generation sites at a level of 0.1%. The lifetime of excited electrons in the metastable state of generation sites was set to be 10^{-8} s. This lifetime was proposed by Samoc and Williams, and applied to kinetic model by Braun to give satisfactory results.^{3,26} The generation efficiency was calculated by,

$$\phi = \phi_0 \frac{\partial \rho / \partial t}{N \cdot S}$$

where ϕ_0 denotes the prefactor, ρ the charge density, N the photon flux density, 3.5×10^{21} photons/($\text{s} \times \text{m}^2$) in this simulation, and S the area of electrode surface. The photocurrent was obtained by summing all the paths traveled along by every mobile hole in unit time.

The sample for the experiment was prepared by blending 1 wt% TNF with 99 wt% PSX-Cz. The photo-charge generation efficiency of TNF/PSX-Cz sample was determined using the xerographic discharge technique.²⁷ Light source of 632.8 nm was irradiated at 0.1 w/cm^2 . The photo-charge generation efficiency ϕ was calculated from the slope of the discharge rate as,

$$\phi = -\frac{C}{eN_0} \left(\frac{dV}{dt} \right)_{vi} = -\frac{\varepsilon\varepsilon_0}{eNl} \left(\frac{dV}{dt} \right)_{vi}$$

where C denotes the capacitance of the sample, N_0 the absorbed photon flux, (dV/dt) the initial photo-induced discharge slope, and l the thickness of sample. The photocurrent of TNF/PSX-Cz sample was determined using simple DC method.²⁸

Results and Discussion

The field dependence of photo-charge generation was examined by our new calculation method. Our simulations were compared to the Onsager theory that has been successful to describe experimental results. The detailed applications of the Onsager theory were described elsewhere.^{1,2,6,11} In those studies, experimental results for TNF/PVK system were fitted using the Onsager theory when the initial separation, r_o , was determined to be 26 Å. We display our simulation results in Fig. 2(a) along with those of the Onsager theory at two different distances of $r_o = 20$ and 26 Å, and with experimental data obtained for TNF/PSX-Cz system. Our experimental data fits Onsager's theory well when the initial separation was set at 20 Å rather than 26 Å. Difference in the separation seems to be attributed to the energetic disorder produced from the dipole moment of the charge transport matrix PSX-Cz (2.44 D) to *N*-vinylcarbazole (1.94 D).

Simulations are also consistent with results of the Onsager theory^{1,2,9} obtained in the field region of 20 to 100 V/ μm for $r_o = 20$ Å. In our research, the generation efficiency comes out proportional in the logarithm scale to the strength of the applied field in the region of 20 to 200 V/ μm . When a hole in the geminate electron-hole pair hops into the nearest

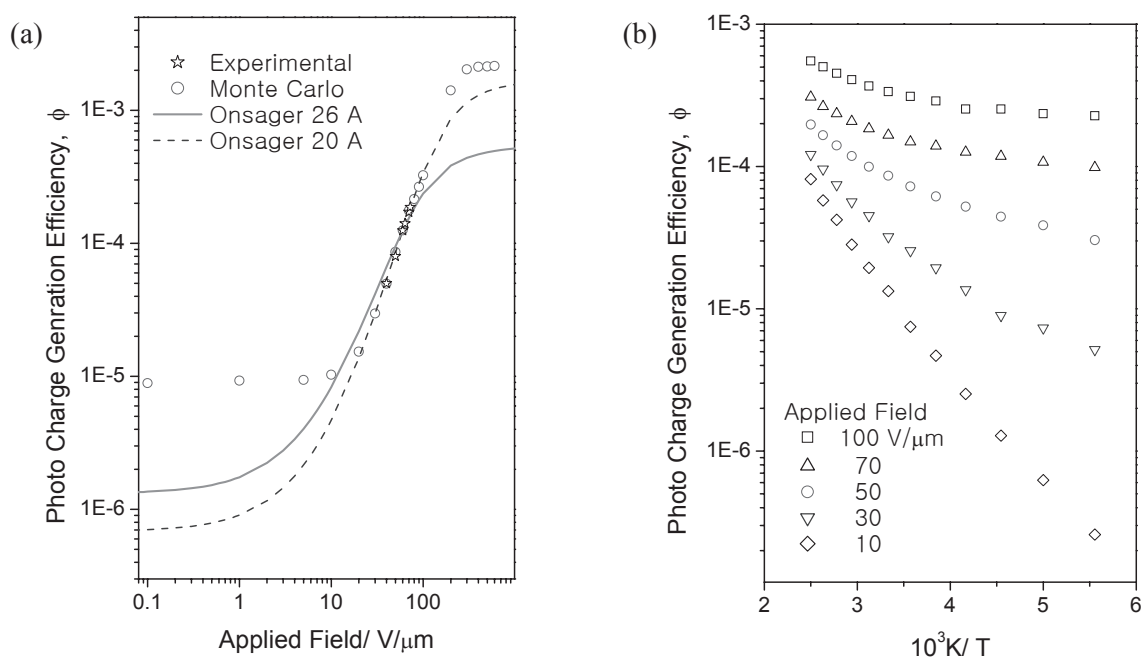


Figure 2. (a) The field dependence of the photo charge generation efficiency. Blank stars; experimental results in TNF/PSX-Cz, Solid line; Onsager's theory with $r_0 = 26 \text{ \AA}$ and $\phi_0 = 5.00 \times 10^{-3}$, Dash line; Onsager's theory with $r_0 = 20 \text{ \AA}$ and $\phi_0 = 1.74 \times 10^{-3}$, Blank dots; our simulation with $r_0 = 20 \text{ \AA}$ and $\phi_0 = 5.34 \times 10^{-5}$ at 300 K. (b) The temperature dependence of the photo charge generation efficiency at various fields with $r_0 = 20 \text{ \AA}$ and $\phi_0 = 5.34 \times 10^{-5}$.

neighboring site, the energy change was calculated by the following, $eEr_0 - \frac{1}{4\pi\epsilon\epsilon_0} \frac{e^2}{r_0}$. When the energy gain (eEr_0) due to hopping in the field of high E is larger than the coulomb potential energy, the hopping rate is saturated by Miller-Abrahams theory. Then, the generation efficiency also reaches a maximum plateau as shown in Fig. 2(a). Also, it reaches a limiting efficiency stage earlier with increasing the initial separation distance. At the low field, it shows a flat region with a deviation of about one order in efficiency from Onsager's. The efficiency decreases rather abruptly to a low-lying steady region while it does smoothly in Onsager's. It would reflect an inability to overcome the coulomb potential barrier for hopping at the low field. Although our predictions are not consistent with Onsager's at the low field, they are in good agreement in the electric field region usually applied in experimental conditions.

Fig. 2(b) shows the temperature dependence of generation efficiency at various strengths of the field in the temperature region 180 to 400 K. It represents a type of sub-Arrhenius temperature dependence as compared with Arrhenius of the Onsager theory.^{2,6} At the low field, the efficiency is very sensitive to temperature because it has inadequate driving forces to cross the barrier. At the high field, however, it is relatively immune to temperature, particularly in the region of low temperature. At high temperature, it varies with temperature. Albrecht and Bässler reported that the energetic disorder could develop the dissociation of geminate electron-hole pairs and consequently gives rise to sub-Arrhenius temperature dependence for the efficiency.¹² Disorder in conducting matrix could develop a broad distribution of site energies and then more carriers are trapped. With decreasing temperature, the

hopping rate becomes reduced. Even though the geminate recombination rate is kept constant, the dissociation efficiency of geminate electron-hole pairs increases as much as the trapped carriers. At the same time, the carriers seized in traps would have less probability to recombine with other independently generated carriers. This reduces the rate of the distant-pair (non-geminate) recombination process. As a result, this process would enhance the efficiency leading to a sub-Arrhenius type.

Two modes have been considered to characterize the physical properties of organic photo conducting devices in theory, i.e. the charge generation and the carrier mobility. To date, the photocurrent in conducting devices could be calculated by association of two modes independently obtained. To predict the photocurrent as well as the photo charge generation, our new calculation adapted the MC method employing multiple site excitation and interaction. This method could enable to monitor all the traces or trajectories of holes writhing or drifting. The field dependence of simulated photocurrents in the present study is shown in Fig. 3(a) with experimental values obtained for TNF/PSX-Cz system. The photocurrent shows proportional dependence in the logarithm scale against the field in the range of 20 to 200 $V/\mu\text{m}$ that is similar in appearance to the efficiency in Fig. 2(a) as a whole.

The temperature dependence of photocurrent has been studied to determine the dominant recombination mechanisms in various temperature regions in terms of the mobility and the carrier density for crystalline²⁹ and polymer systems.^{30,31} The photocurrent in this simulation work is displayed in Fig. 3(b) as a function of $1/T$ in the temperature region 180 to 400 K, which presents an Arrhenius type dependence. It could be inferred from this feature that mixed effects of the carrier mo-

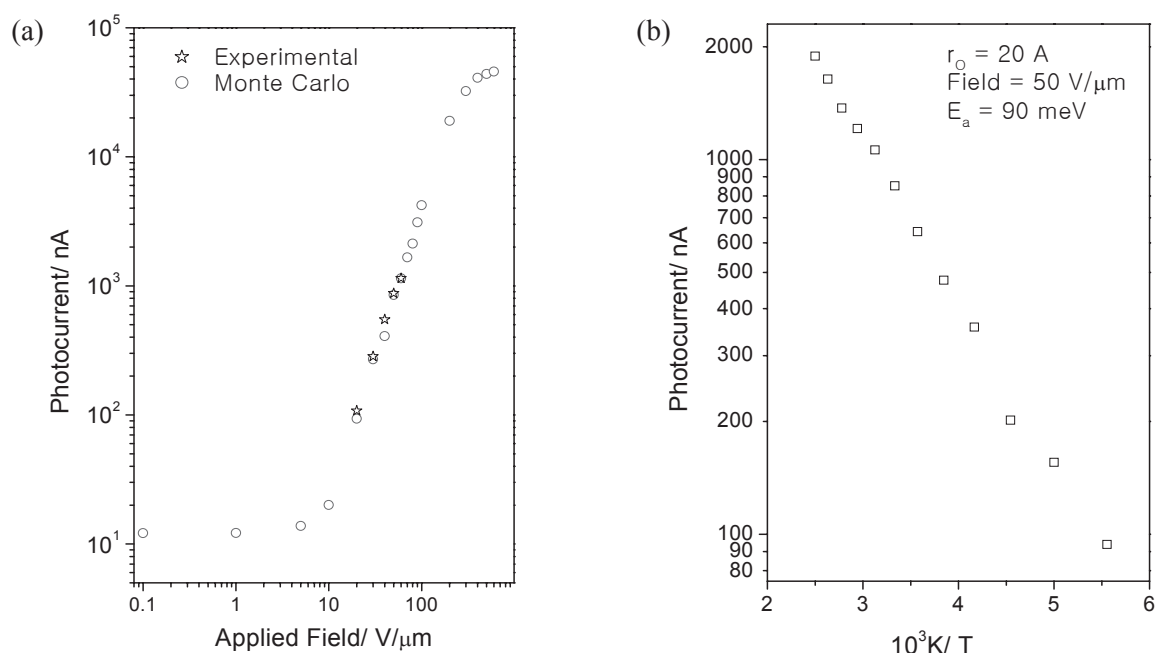


Figure 3. (a) The field dependence of the photocurrent. Blank stars; experimental results of TNF/PSX-Cz, Blank dots; our simulation with $r_0 = 20 \text{ \AA}$ at 300 K. (b) The temperature dependence of the photocurrent calculated with $r_0 = 20 \text{ \AA}$ and applied field = $50 \text{ V}/\mu\text{m}$.

bility and charge generation produce a certain amount of photocurrent in a complementary manner, and consequently to show the same activation energy throughout. The photocurrent is thermally activated rate dependent on the applied field and reaches a steady stage rather slowly. It implies that transporting phenomena of carriers suffer from the presence of shallow and increased traps indicating an enhanced energetic disorder in the matrix. Also, the dissociation of geminate pairs can be affected with temperature to modulate the carrier density. In the photo charge generation, the energetic disorder could enhance the generation efficiency through increased trapped holes. However, it does not raise the photocurrent as much as in the case of the efficiency because the thermal or forced releasing process of trapped carriers is restricted, especially at low temperature.

The sensitizer concentration dependence of the photo-

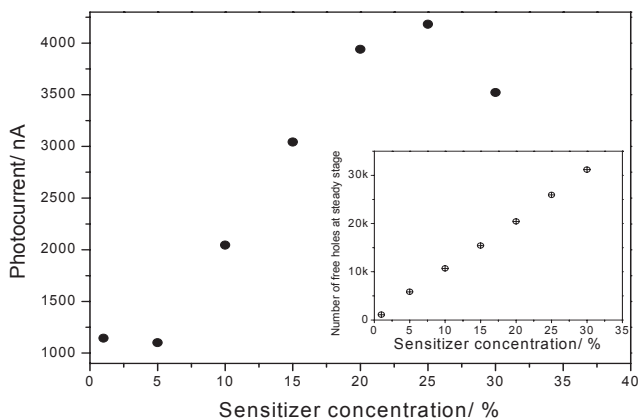


Figure 4. The sensitizer concentration dependence of the photocurrent with $r_0 = 20 \text{ \AA}$ and applied field = $50 \text{ V}/\mu\text{m}$. The inset is the number of free holes upon the sensitizer concentration at the steady stage with $r_0 = 20 \text{ \AA}$ and applied field = $50 \text{ V}/\mu\text{m}$.

current was shown in Fig. 4. The holes would increase with the sensitizer, but the photocurrent shows a maximum at 25% of sensitizer concentration. This agrees with experimental result of (2,4,7-trinitro-9-fluorenylidene)-malononitrile in PVK system by Steenwinckel and et al.³² where the elevated concentration of sensitizer could work as traps to suppress the hole mobility. The space charge field formation was similarly dependent on the disorder of the matrix with dipolar materials at the steady stage.¹⁹ The amount of sensitizer could increase the concentration of holes, but the photocurrent would reach a maximum due to suppressed hole mobility caused by increased energetic disorder in the matrix.

Conclusions

A new approach for the photo charge generation efficiency and the photocurrent in photoconductive polymer system was proposed using the MC simulation method. This method employed the multiple site generation and counted the interactions of carriers with other charges within Coulomb radius during migration of holes through the matrix. In this work, we adapted the energetic disorder of the correlation disorder model to facilitate the introduction of dipole moment into simulation. The inhomogeneous distribution of charge carriers was created by multiple site generation of photo-induced charges. Their interactions during migration of holes with other charges in moving boundary of Coulomb sphere were explicitly counted as an additional energetic disorder.

This method predicts well the generation efficiency and photocurrent simultaneously in the span of experimentally applied field, 20 to $200 \text{ V}/\mu\text{m}$. This also describes properly the sensitizer concentration dependence of the photocurrent as shown in Fig. 4. Although our method presents the role of the initial charge separation insufficiently, our model demon-

strates the details of photo charge generation efficiency and photocurrent in organic photoconductive devices. Particularly, this method can be applied for incorporated features of the charge generation and migration in organic photoconductive devices where geminate electron-hole pairs are randomly dispersed in the matrix.

Acknowledgments. This work was supported by the Korea Science and Engineering Foundation (KOSEF) grant funded by the Korea government (MEST) (No. R11-2007-050-01003-0). We also wish to thank Brain Korea 21 for the financial support.

References

- Melz, P. J. *J. Chem. Phys.* **1972**, *57*, 1694.
- Borsenberger, P. M.; Ateya, A. I. *J. Appl. Phys.* **1978**, *49*, 4035.
- Braun, C. L. *J. Chem. Phys.* **1984**, *80*, 4157.
- Goliber, T. E.; Perlstein, J. H. *J. Chem. Phys.* **1984**, *80*, 4162.
- Cimrová, V.; Nešpůrek, A. *Chem. Phys.* **1994**, *184*, 283.
- Lin, L.-B.; Jenekhe, S. A.; Borsenberger, P. M. *J. Chem. Phys.* **1996**, *105*, 8490.
- Miyasaka, H.; Moriyama, T.; Ide, T.; Itaya, A. *Chem. Phys. Lett.* **1988**, *292*, 339.
- Jung, J.; Głowacki, I.; Ulański, J. *J. Chem. Phys.* **1999**, *110*, 7000.
- Głowacki, I.; Jung, J.; Ulański, J. *Synth. Met.* **2000**, *109*, 143.
- Onsager, L. *J. Chem. Phys.* **1934**, *2*, 599.
- Onsager, L. *Phys. Rev.* **1938**, *54*, 554.
- Albrecht, U.; Bäessler, H. *Chem. Phys. Lett.* **1995**, *235*, 389.
- Barth, S.; Herter, D.; Tak, Y.-H.; Bäessler, H.; Hörhold, H. H. *Chem. Phys. Lett.* **1997**, *274*, 165.
- Offermans, T.; Meskers, S. C. J.; Janssen, R. A. J. *J. Chem. Phys.* **2003**, *119*, 10924.
- Pasveer, W. F.; Cottaar, J.; Tanase, C.; Coehoom, R.; Bobbert, P. A.; Blom, P. W. M.; Leeuw, D. M. de; Michels, M. A. J. *Phys. Rev. Lett.* **2005**, *94*, 206601.
- Baranovskii, S. D.; Rubel, O.; Thomas, P. *Thin Solid Films* **2005**, *487*, 2.
- Offermans, T.; Meskers, S. C. J.; Janssen, R. A. J. *Chem. Phys.* **2005**, *308*, 125.
- Lee, C. J. *Bull. Korean Chem. Soc.* **2006**, *27*, 1186.
- Lee, C.; Yang, M.; Lee, N.-S.; Kim, N. *Chem. Phys. Lett.* **2006**, *418*, 54.
- Lee, C.; Park, S.-K.; Yang, M.; Lee, N.-S.; Kim, N. *Chem. Phys. Lett.* **2006**, *422*, 106.
- Lee, C.; Park, S.-K.; Yang, M.; Lee, N.-S.; Kim, N. *Bull. Korean Chem. Soc.* **2007**, *28*, 447.
- Novikov, S. V.; Vannikov, A. V. *Synth. Met.* **1997**, *85*, 1167.
- Novikov, S. V.; Dunlap, D. H.; Kenkre, V. M.; Pattis, P. E.; Vannikov, A. V. *Phys. Rev. Lett.* **1998**, *81*, 4472.
- Miller, A.; Abrahams, E. *Phys. Rev.* **1960**, *120*, 745.
- Schönherr, G.; Bäessler, H.; Silver, M. *Phil. Mag. B* **1981**, *44*, 47.
- Samoc, M.; Willams, D. F. *J. Chem. Phys.* **1983**, *78*, 1924.
- Borsenberger, P. M.; Weiss, D. S. *Organic Photoreceptors for Imaging Systems*; Marcel Dekker Inc.: New York, 1993.
- Schildkraut, J. S. *Appl. Phys. Lett.* **1991**, *58*, 340.
- Ito, C.; Kigoshi, S. *Phys. Stat. Sol. A* **2006**, *203*, 3774.
- Gommans, H. H. P.; Kemerink, M.; Kramer, J. M.; Janssen, R. A. J. *Appl. Phys. Lett.* **2005**, *87*, 122104.
- Mihailetchi, V. D.; Koster, L. J. A.; Hummelen, J. C.; Blom, P. W. M. *Phys. Rev. Lett.* **2004**, *93*, 216601.
- Steenwinckel, D. V.; Hendrickx, E.; Persoons, A. *J. Chem. Phys.* **2001**, *114*, 9557.